American Mineralogist, Volume 86, pages 1513–1518, 2001

Crystal structures of Na and K aluminate mullites

REINHARD X. FISCHER,[1,*] MARTIN SCHMÜCKER,[2] PAUL ANGERER,[2] AND HARTMUT SCHNEIDER[2]

[1]Fachbereich Geowissenschaften der Universität, Klagenfurter Strasse, D-28359 Bremen, Germany
[2]Deutsches Zentrum für Luft- und Raumfahrt, Institut für Werkstoff-Forschung, D-51147 Köln, Germany

ABSTRACT

Mullite-type alkali aluminates $(K_yNa_{1-y})_{0.67}Al_6O_{9.33}$ were synthesized from amorphous Al and alkali nitrates by sol-gel techniques. Rietveld refinements of six members of the solid solution series (y = 0.0, 0.2, ..., 1.0), together with Fourier syntheses and grid search analyses show that the Na and K atoms reside in the vacant Oc sites, with K at 1/2, 0, 1/2 and Na on a split site off the special position. The number of alkali atoms is restricted to 2/3 atoms per unit cell due to crystal chemical constraints. Consequently, unlike the aluminosilicate mullites, alkali mullites do not form a solid solution series with varying oxygen composition. All compounds studied here crystallize in space group *Pbam* with lattice constants ranging from $a = 7.6819(4)$ Å, $b = 7.6810(4)$ Å, $c = 2.91842(8)$ Å for the Na aluminate to $a = 7.6934(3)$ Å, $b = 7.6727(3)$ Å, $c = 2.93231(7)$ Å for the K aluminate mullite.

INTRODUCTION

The mullite-type structure family is characterized by AlO_6 octahedra that share edges to form chains running parallel to the crystallographic **c** axis. The chains are cross-linked by double chains of TO_4 tetrahedra with a random distribution of Al and Si atoms on the T site. Since some Si is substituted by Al, oxygen vacancies form to retain charge balance. The amount of Si → Al substitution and correlated oxygen vacancy formation is variable according to the general formula $Al_2(Al_{2+2x}Si_{2-2x})O_{10-x}$. The x value ranges between approximately 0.2 and 0.5 (Burnham 1964a; Angel and Prewitt 1986). According to Burnham (1964b) the crystal structure of mullite fits any composition between sillimanite ($x = 0$) and ι-Al_2O_3 ($x = 1$). However, the aluminate end-member has not yet been observed, although mullite related phases with $x > 0.9$ have been described (Schneider et al. 1993; Fischer et al. 1994).

Mullite-type alkali aluminate phases were first synthesized by Perrotta and Young (1974) using sol-gel techniques. They observed the formation of mullite-type phases of good crystallinity after calcination above 950 °C. The compounds occur within a small temperature window; above 1000 °C the mullite-type phases decompose to form α- and β-alumina. Elliot and Huggins (1975) crystallized mullite-type Na-aluminate by ashing filter paper soaked in aqueous salt solutions and heating above 800 °C. The resulting compound was designated as λ-$Na_2O{\cdot}x\ Al_2O_3$ with x ranging between 3 and 12. Elliot and Huggins (1975) reported that the metastability of the λ-phase strongly depends on an intimate mixing of the reactants. The crystal structure of the Na-aluminate phase was discussed on the basis of the X-ray powder diffraction pattern that is similar to that of mullite. According to Elliot and Huggins (1975) the unit cell is orthorhombic with $a = b$, resulting in a pseudotetragonal metric. The alkali aluminate structure proposed by them corresponds to that of mullite with alkali ions occupying the Oc site at 0, 1/2, 1/2. It was mentioned that the substitution of Na by K leads to a better geometrical fit, since K has an ionic radius which is nearly identical to that of oxygen while Na is somewhat smaller. More recently, Mazza et al. (1992) published detailed data for mullite-type phases with compositions $Na_2O{\cdot}6Al_2O_3$ and $K_2O{\cdot}6Al_2O_3$, respectively. They confirmed the structural model given by Elliot and Huggins (1975). However, the alkali atom positions, the distribution of Al atoms in the aluminate tetrahedra, and the general compositions of the compounds seem to be doubtful because they do not agree with the crystal chemical constraints imposed by the local symmetry of the alkali and O atom positions as discussed in the results and discussion section. Possible synthesis routes for the alkali aluminates are oxalate coprecipitation or alkoxide and nitrate decomposition. It was confirmed that the mullite-type compounds transform to stable β-alumina above 1000 °C.

In the present study, we have synthesized Na and K aluminates with mullite-type structures to determine the alkali atom positions and to explain the chemical composition by crystal chemical considerations.

EXPERIMENTAL METHODS

Synthesis of aluminate compounds with mullite-type structure

The synthesis of the aluminate compounds was performed according to the method of Mazza et al. (1992). To begin with, a noncrystalline precursor was prepared that transformed into the crystalline phase after calcination at 950 °C. The noncrystalline precursor was synthesized by decomposition of Al- and alkaline nitrates. Beginning with a stoichiometric mixture of

* E-mail: rfischer@min.uni-bremen.de

$Al(NO_3)_3 \cdot 9H_2O$ and alkaline nitrates, a small amount of water and 10 to 20% glycerol (1,2,3-propantriol, $C_3H_8O_3$) as a reduction agent were added. After homogenization the reaction mixture was heated carefully and constantly stirred until solution of the nitrates and formation of a homogenous liquid phase was complete. With increasing temperature the mixture foamed up and the development of CO and CO_2 was observed. At 110 °C decomposition of the nitrates began and the color of the nitrous oxides containing developing vapors changed to brownish red. The reaction follows the general scheme:

$$2Me^{+}NO_3 + 18Al(NO_3)_3 \cdot 9H_2O + 6C_3H_8O_3 + 7O_2 \rightarrow 3Me^{+}_{0.67}Al_6O_{9.33} + 56NO_2\uparrow + 18CO_2\uparrow + 186H_2O.$$

The viscosity of the reaction product increased during the decomposition process resulting in a spongy mass after drying.

X-RAY ANALYSIS AND RIETVELD REFINEMENTS

X-ray diffraction data collection was performed with a Philips X'Pert diffractometer with a Ge monochromator in the primary beam yielding a strictly monochromatic radiation. Details of data collection, crystallographic data, and definitions are given in Table 1. The background was fitted by linear interpolation between reference points set by hand. Intensities within eight times the full width at half maximum of a peak were considered to contribute to the central reflection. Peaks below 50° 2θ were corrected for asymmetry effects using Rietveld's (1969) algorithm. The pseudo-Voigt function was used for the simulation of the peak shape, with a refinable parameter defining the Lorentzian and Gaussian character of the peaks as a function of 2θ. The Rietveld analysis (Rietveld 1969) was performed with a modified version of the PC-Rietveld plus package (Fischer et al. 1993). X-ray scattering factors in their respective valence states were taken from the *International Tables for X-ray Crystallography* (Ibers and Hamilton 1974) and the values for O^{2-} from Hovestreydt (1983). The crystal structure drawings were performed with a modified version of the STRUPLO program (Fischer and Messner 2001).

RESULTS AND DISCUSSION

Structural data (atomic positions, displacement factors, site symmetry, Wyckoff positions and occupancies) obtained by X-ray analysis and subsequent Rietveld refinement are listed in Table 2, and selected interatomic distances are given in Table 3. The fit between observed and calculated intensities of X-ray diffraction diagrams is shown in Figures 1 and 2. The Rietveld analysis of the X-ray diffraction data confirmed that the crystal structure of alkali aluminate mullites consists of AlO_6 octahedra, which form chains linked by Al_3O groups (tricluster) in the (001) plane as shown in Figures 3 and 4. The alkali atoms are located unambiguously in the cavities of the oxygen (Oc) vacancies in or close to 1/2, 0, 1/2. This has been confirmed by Fourier synthesis and grid search analyses, a method to determine atom positions described by Baur and Fischer (1986). Without the alkali atoms on the Oc position, the refinements yielded negative displacement parameters for Oc* [(–3.9(1) Å^2 for K-mullite, –2.8(2) Å^2 for Na-mullite)] and after introducing the alkali atoms, the residuals dropped from R_{wp} = 14.1%

TABLE 1. Experimental conditions, crystallographic data, and definitions used in data refinement

	Philips X'Pert
Radiation type, source	X-ray, Cu$K\alpha_1$
Discriminator	primary beam, germanium monochromator
Divergence slit	0.25°
Receiving slit	0.2 mm
Data collection temperature	room temperature
2θ range used in refinement	10 – 140°
Step size	0.03°
Counting time per step	35 s for all samples except K-aluminate (y = 0) with 100 s due to small amount of sample
Space group	*Pbam*
Z	1

Lattice parameters (Å) in compounds of the solid solution series $(K_yNa_{1-y})_{0.67}Al_6O_{9.33}$

	a	*b*	*c*
y = 0	7.6819(4)	7.6810(4)	2.91842(8)
y = 0.2	7.6831(4)	7.6789(4)	2.92153(9)
y = 0.4	7.6843(4)	7.6781(3)	2.92487(8)
y = 0.6	7.6869(4)	7.6782(3)	2.92800(8)
y = 0.8	7.6916(4)	7.6757(3)	2.93103(9)
y = 1	7.6934(3)	7.6727(3)	2.93231(7)

Residuals (%)	*Rwp*	*R'$_p$*	*R$_e$*	*R$_B$*
y = 0	9.5	17.7	2.2	4.3
y = 0.2	11.3	18.2	2.0	9.1
y = 0.4	9.8	16.8	2.0	6.5
y = 0.6	9.8	17.1	2.1	6.1
y = 0.8	10.4	18.4	2.1	7.3
y = 1	8.7	17.4	2.2	5.3

Definitions: $R_{wp} = \sqrt{\frac{\sum_i (y_{io} - C \cdot y_{ic})^2}{\sum_i w_i y_{io}^2}}$ $R_p' = \frac{\sum_i | y_{io} - C \cdot y_{ic} |}{\sum_i | y_{io} - y_{ic} |}$ $R_e = \sqrt{\frac{N-P}{\sum_i w_i y_{io}^2}}$ $R_B = \frac{\sum_k | I_{ko} - C \cdot I_{kc} |}{\sum_k I_{ko}}$.

TABLE 2. Positional parameters, isotropic displacement factors (Å^2), site symmetry, Wyckoff position, and occupancies

Atom	*x*	*y*	*z*	*B*	Site symm.	Wyckoff pos.	No. of atoms per unit cell
Na	0.087(3)	0.561(3)	1/2	1.4(5)	. . m	4h	0.67 Na
K	0	_	1/2	2.7(1)	. . m	2d	0.67 K
M1(Al)	0	0	0	0.79(5)	. . 2/m	2a	2
	0	0	0	1.02(5)			
T(Al)	0.1510(5)	0.3331(5)	1/2	0.83(6)	. . m	4h	2.67
	0.1543(4)	0.3300(3)	1/2	0.82(5)			
T*(Al)	0.2691(8)	0.1956(9)	1/2	1.1(2)	. . m	4h	1.33
	0.2678(6)	0.1918(7)	1/2	0.9(1)			
Oab	0.3602(6)	0.4211(5)	1/2	1.31(9)	. . m	4h	4
	0.3622(4)	0.4178(4)	1/2	1.50(8)			
Oc*	0.4843(32)	0.0458(19)	1/2	1.1(4)	. . m	4h	1.33
	0.4412(14)	0.0525(15)	1/2	0.4(2)			
Od	0.1318(7)	0.2124(5)	0	1.2(1)	. . m	4g	4
	0.1346(4)	0.2078(4)	0	1.2(1)			

Note: First line corresponds to Na aluminate mullite (y = 0), second line to K aluminate mullite (y = 1). Data for site symmetry and Wyckoff position taken from the *International Tables of Crystallography* (Hahn 1983). Oc* is the bridging oxygen atom in the tricluster of the $T_2T^*Oc^*$ groups consisting of two TO_4 and one T^*O_4 group.

TABLE 3. Selected interatomic distances (Å)

(a) Na mullite (y = 0)								
Na – Oab	2.46(2)	4 × M1-Oab	1.910(3)	T – Oc*	1.583(22)	2 × T* - Od	1.805(5)	
Na – Oab	2.80(2)	2 × M1-Od	1.920(4)	2 × T – Od	1.735(3)	T* - Oab	1.868(8)	
2 × Na – Od	2.83(2)			T – Oab	1.744(6)	T* - Oc*	2.014(23)	
2 × Na – Od	2.86(2)							
2 × Na – Od	3.07(2)							
		mean	1.913	mean	1.699	mean	1.873	
(b) K mullite (y = 1)								
2 × K – Oab	2.857(3)	2 × M1-Od	1.901(3)	T – Oab	1.736(4)	T – Oc*	1.709(12)	
4 × K – Od	2.872(3)	4 × M1-Oab	1.916(2)	2 × T – Od	1.747(2)	2 × T* - Od	1.793(3)	
				T* - Oc*	1.859(11)	T* - Oab	1.880(6)	
		mean	1.911	mean	1.772	mean	1.794	

to 8.7% and R_B = 17.6% to 5.3% for the K-mullite, and R_{wp} = 11.2% to 9.5% and R_B = 9.6% to 4.3% for the Na-mullite, and all atomic displacement parameters were positive.

The K atoms are located exactly in the center of the cavities at 1/2, 0, 1/2, whereas the smaller Na atoms are shifted on the long axis of the elliptical cavity closer to the O atoms of the aluminate polyhedra. The offset of the Na atom from the 2*d* site at 1/2, 0, 1/2 implies that this position is split into two symmetrically equivalent positions in 4*h* which are too close to each other for simultaneous occupancy. The Na atoms shown in Figure 3 are arbitrarily placed on one of the two split positions.

In contrast to our findings, Mazza et al. (1992) placed both Na and K atoms on the Oc* positions and they located the O atoms bridging adjacent tetrahedra in the special Oc position. The sum of the occupancies of the O (O3 and O4 in Mazza et al. 1992) and alkali atoms in the local environment of this position is given as 1.5 O + 1.0 (Na, K) and therefore exceeds the theoretically possible number of two atoms per unit cell. This limit of two atoms results from the local 2/*m* symmetry of the 2*d* site (Hahn 1983) which yields a split position when an atom is displaced from 1/2, 0, 1/2. Only one of the two atoms in this split position can be occupied because of the short distance between the split partners. Our refinements revealed that K resides in the vacant Oc site (1/2, 0, 1/2) and Na is shifted closer to the O atoms of the AlO_6 octahedra. This reflects the different ionic radii of Na and K with smaller Na-O than K-O bond lengths.

It was not possible to determine the chemical composition of the nano-sized alkali aluminate crystals analytically due to the multiphase composition of the sample. Therefore, we used a crystal chemical approach to determine the structural state *x* of the alkali aluminates. The chemical composition of Al,Si-mullites is given by the formula $Al_2(Al_{2+2x}Si_{2-2x})O_{10-x}$. In mullite-type aluminates where all Si^{4+} ions are replaced by Al^{3+} a (Al_6O_{10-x}) substructure with a negative charge of 2–2*x* emerges. To achieve charge balance this negative charge has to be compensated by incorporation of an equivalent number (2–2x) of positively charged cations leading to an alkali aluminate composition of $(Na,K)_{2-2x}Al_6O_{10-x}$. Considering that the number of atoms in the vicinity of 1/2, 0, 1/2 must not exceed the multiplicity of the 2*d* site as explained above, only 2/3 Na or K atoms can be placed on this site yielding a composition of $(Na,K)_{2/3}Al_6O_{10-2/3}$ or $(Na,K)_{0.67}Al_6O_{9.33}$ (x = 0.67). This results from the sum of (Na,K), Oc, and Oc* atoms which must not exceed 2 atoms per unit cell. An *x* value <2/3 yields 2–3*x* Oc + 2*x* Oc* + 2–2*x* (Na,K) (see Table 6 in Fischer et al. 1994) which is 4–3*x* atoms per unit cell and consequently >2 for x < 2/3. An *x* value >2/3 requires the formation of T_4O groups which is energetically unfavorable, and is only observed in the metastable high alumina mullites described by Fischer et al. (1996). The upper limit of the number of alkali atoms that can be placed in the cavities can also easily be derived from the crystal structure projections shown

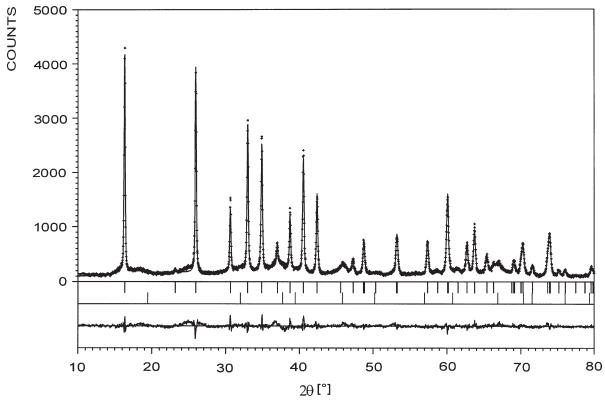

FIGURE 1. Observed (crosses) and calculated (solid line) powder patterns with difference curves underneath. Peak positions permitted by the cell metric are indicated by tick marks (1st row: Na mullite, 2nd row: γ-Al_2O_3).

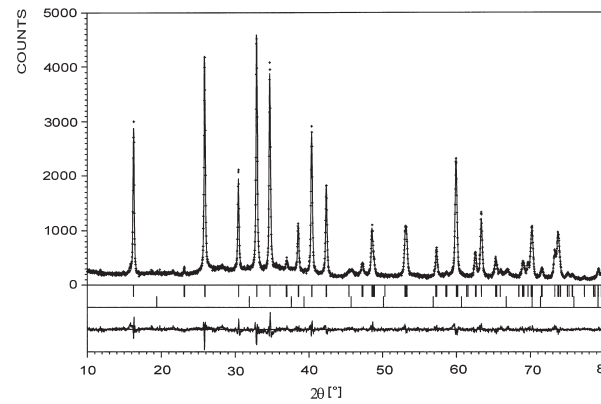

FIGURE 2. Powder pattern of K mullite as described in Figure 1.

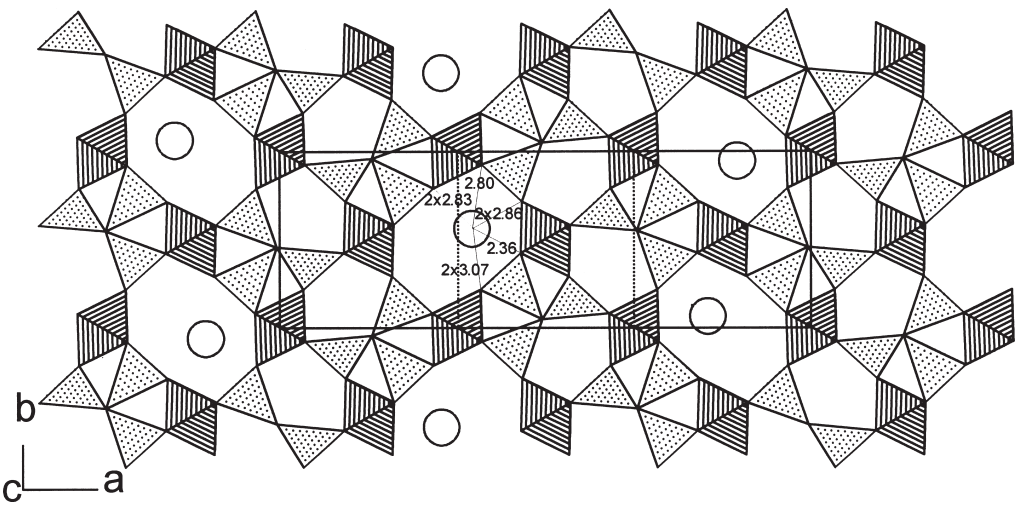

FIGURE 3. Crystal structure projection of the local mullite structure presented in a hypothetically ordered $3 \times a$ supercell as described in Fischer et al. (1994). The real structure is represented by the superposition of all possible settings of the small cells. The Na atoms are shown as circles on one of the two split sites with their distances to the next nearest O atoms of the aluminate polyhedra.

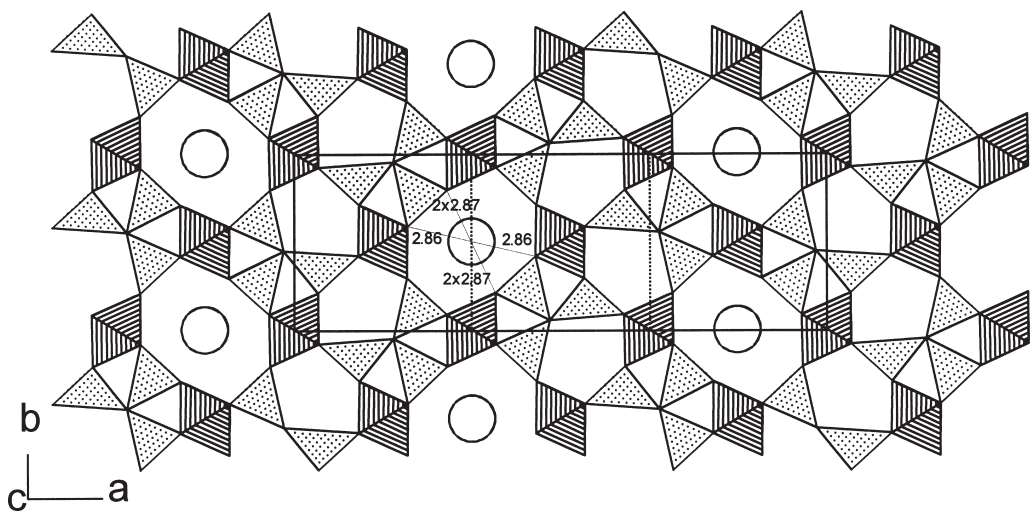

FIGURE 4. Crystal structure projection of the K mullite in a setting according to Figure 3.

in Figures 3 and 4. They show a hypothetically ordered mullite with framework composition $Al_6O_{9.33}$. Thus, the crystal structure models shown in these figures represent one of various local arrangements of the mullite structure of this composition. The average structure yielding the diffraction pattern corresponds to the superimposed unit cells with a statistical distribution of the tetrahedrally coordinated Al, and the (Na,K) and Oc* atoms on four [T, T*, (Na,K), Oc*] sites. However, all possible arrangements of tetrahedral linkages will give a framework structure with two large voids (cavity A in Fischer et al. 1994) in the triple cell giving space for two interstitial cations. Consequently, the number of alkali atoms cannot exceed 2 atoms in the triple cell or 2/3 in the real cell of mullite.

The solid solution series between the mullite-type K and Na aluminate end-members has been studied by Rietveld refinement. However, due to the proximity of K, Na, and Oc* on split positions around the 2*d* position, and the close proximity (between 1.6 and 1.5 Å) to T and T*, respectively, the correlations between positional and atomic displacement parameters of the corresponding atoms are too high for an accurate determination of the atomic positions in the average structure. Therefore, Na and K positions were fixed at their respective values from the end-member refinements (0.087, 0.561, 0.5 and 0.0, 0.5, 0.5) and the occupancies were set according to the Na/K ratio of the bulk composition. Since we do not know the amount of alkalis incorporated in the possibly coexisting amorphous phase, the real Na/K distribution in the mullite phase might deviate slightly from this setting. However, the resulting lattice constant refinements clearly indicate that the Na and K mullites form a continuous solid solution series (Fig. 5). With increasing K content, the *a* and *c* lattice constants increase whereas the *b* parameter decreases.

The nonisotropic change of lattice constants caused by K↔Na substitution can be rationalized by Figure 6 showing the Na- and K-environments in the respective mullite-type structures. As mentioned above, an atomic position close to the Oc

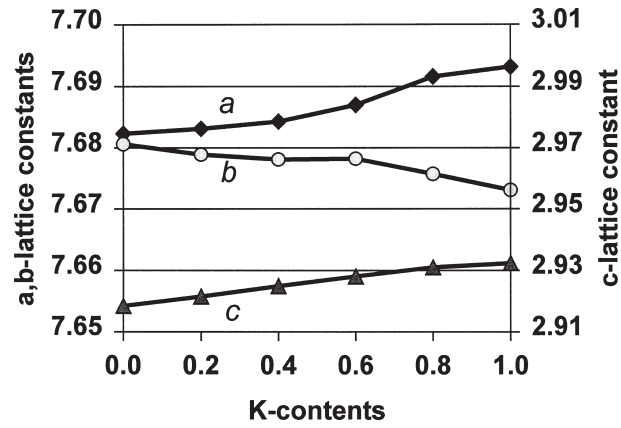

FIGURE 5. Lattice constants of the alkali mullites in the solid solution series $(Na_yK_{1-y})_{0.67}Al_6O_{9.33}$.

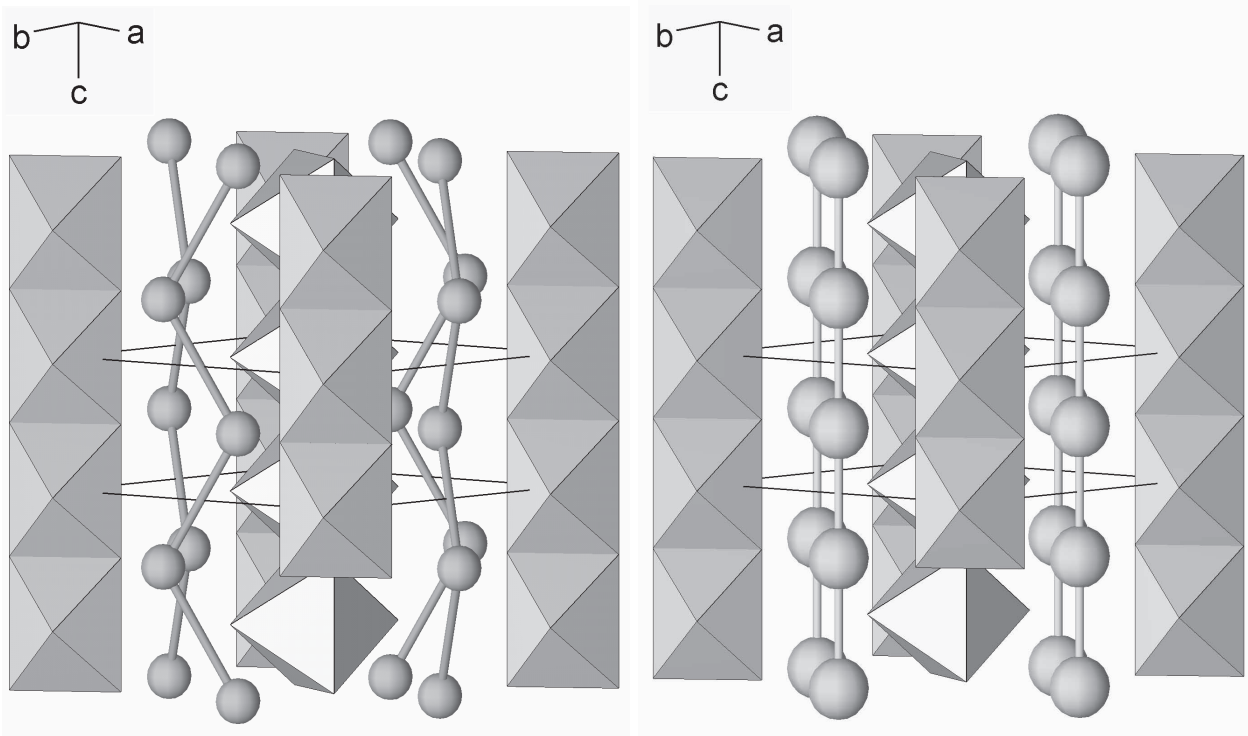

FIGURE 6. Crystal structure projections of alkali aluminate mullites projected with **c** in the plane of drawing. Only the ordered AlO_6 octahedral chains parallel **c** and the alkali atom positions are shown. One octahedron in the front is omitted. The alkali atoms are drawn with half the size of their effective ionic radii (Shannon 1976). It should be noted that the sticks between the alkali atoms only indicate the geometrical alignment of the atoms, they do not represent atomic bonds. Only one out of three alkali atom positions is actually occupied by alkali atoms. (**a**) Na-aluminate mullite. Four zigzag chains of Na atom positions are shown, each representing one of the two possible split positions. (**b**) K-aluminate mullite with four chains of ordered K-atom positions.

vacancy (oxygen vacancy position OVP) can be occupied by one atom only, i.e., either by the O atom itself (Oc*), or by one Na or K atom. The slightly different sites for Na and K in the aluminate structure may influence the alignment of these atoms in the **c** direction. In the case of the Na-aluminate a zigzag-shaped alignment of OVP atoms is possible (Fig. 6a) whereas for the K-aluminates no or only a very small displacement perpendicular to the **c** axis is allowed for the respective atoms, giving rise to an almost linear OVP site alignment (Fig. 6b). Thus, if Na atoms are substituted by K atoms, two factors become effective; the radius of the alkali ion increases and the alignment of OVP atoms along the **c** axis has to be virtually linear. The size effect alone would not necessarily produce intensive *c parameter* expansion, if a zigzag OVP alignment would be possible or, in other words, if the OVP-OVP bonding vector has a significant component in the *a*-*b* plane. In contrast to Na aluminates a distinct zigzag OVP alignment does not occur in K-aluminates and consequently the *c* parameter has to increase superproportionally as a response on the substitution of Na by bigger K ions. The relatively large expansion of the *c* parameter caused by the K ↔ Na substitution corresponds to the stretching of the bond lengths between the K atom (z = 1/2) and Od (z = 0). As a consequence, the *a* and *b* components of this vector should decrease. Our finding of decreasing **b** axis when Na is replaced by K supports this idea considering that the *b* component of the K-Od bond vector is predominant with respect to the *a* component. The *a* parameter, however, becomes larger when Na is substituted by K. This can be explained in terms of the alkali-Oab (z = 1/2) bond vector which is parallel to **a** in a first order approximation and hence is not affected by the above mentioned increase of the *c* parameter.

REFERENCES CITED

Angel, R.J. and Prewitt, C.T. (1986) Crystal structure of mullite: A re-examination of the average structure. American Mineralogist, 71, 1476–1482.

Baur, W.H. and Fischer, R.X. (1986) Recognition and treatment of background problems in neutron powder diffraction refinements. In Barrett, C.S., Cohen, J.B., Faber, J., Jenkins, R., Leyden, D.E., Russ, J.C., and Predecki, P.K., Eds., Advances in X-ray Analysis, vol. 29, p. 131–142. Plenum Publishing Corporation, New York.

Burnham, C.W. (1964a) Crystal structure of mullite. Carnegie Institution of Washington Yearbook, 63, 223–227.

———(1964b) Composition limits of mullite and the sillimanite–mullite solid solution problem. Carnegie Institution of Washington Yearbook, 63, 227–228.

Elliot, A.G. and Huggins, R.A. (1975) Phases in the system $NaAlO_2$-Al_2O_3. Journal of the American Ceramic Society, 58, 497–500.

Fischer, R.X. and Messner, T. (2001) A new version of the STRUPLO program for crystal structure drawings. University of Bremen, Germany.

Fischer, R.X., Lengauer, C., Tillmanns, E., Ensink, R.J., Reiss, C.A., and Fantner, E.J. (1993) PC-Rietveld plus, a comprehensive Rietveld analysis package for PC. Materials Science Forum, 133–136, 287–292.

Fischer, R.X., Schneider, H., and Schmücker, M. (1994) Crystal structure of Al-rich mullite. American Mineralogist, 79, 983–990.

Fischer, R.X., Schneider, H., and Voll, D. (1996) Formation of aluminum rich 9:1 mullite and its transformation to low alumina mullite upon heating. Journal of the European Ceramic Society 16, 109–113.

Hahn, T., Ed. (1983) International tables for crystallography, vol. A, p. 272–273. Kluwer, Dordrecht, The Netherlands.

Hovestreydt, E. (1983) On the atomic scattering factor for O^{2-}. Acta Crystallographica, A39, 268–269.

Ibers, J.A. and Hamilton, W.C., Eds. (1974) International tables for X-ray crystallography, vol. 4, p. 99–149. Kynoch, Birmingham, U.K.

Mazza, D., Vallino, M., and Busca, G. (1992) Mullite-type structures in the systems Al_2O_3-Me_2O (Me = Na, K) and Al_2O_3-B_2O_3 Journal of the American Ceramic Society, 75, 1929–1934.

Perrotta, A.J. and Young, J.E. (1974) Silica-free phases with mullite-type structures. Journal of the American Ceramic Society, 57, 405–407.

Rietveld, H.M. (1969) A profile refinement method for nuclear and magnetic structures. Journal of Applied Crystallography, 2, 65–71.

Schneider, H., Fischer, R.X., and Voll, D. (1993) A mullite with lattice constants $a > b$. Journal of the American Ceramic Society, 76, 1979–81.

Shannon, R.D. (1976) Revised effective ionic radii and systematic studies on interatomic distances in halides and chalcogenides. Acta Crystallographica, A 32, 751–767.

MANUSCRIPT RECEIVED MARCH 13, 2001
MANUSCRIPT ACCEPTED JULY 4, 2001
MANUSCRIPT HANDLED BY BRYAN CHAKOUMAKOS